Doublon-holon excitations split by Hund's rule coupling within the orbital-selective Mott phase

Yuekun Niu,[1] Jian Sun,[2] Yu Ni,[1] Jingyi Liu,[1] Yun Song,[1,*] and Shiping Feng[1]

[1]*Department of Physics, Beijing Normal University, Beijing 100875, China*

[2]*Beijing National Laboratory for Condensed Matter Physics,Institute of Physics, Chinese Academy of Sciences, Beijing 100190, China*

(Received 21 March 2019; revised manuscript received 20 August 2019; published 30 August 2019)

Multiorbital interactions have the capacity to produce an interesting kind of doublon-holon bound state that consists of a single-hole state in one band and a doubly occupied state in another band. Interband doublon-holon pair excitations in the two-orbital Hubbard model are studied by using dynamical mean-field theory with the Lanczos method as the impurity solver. We find that the interband bound states may provide several in-gap quasiparticle peaks in the density of states of the narrow band in the orbital-selective Mott phase with a small Hund's rule coupling (J). There exists a corresponding energy relation between the in-gap states of the narrow band and the peaks in the excitation spectrum of the doublon for the wide band. We also find that the spin-flip and pair-hopping Hund interactions can divide one quasiparticle peak into two peaks, where the splitting energy increases linearly with increasing J. Strong Hund's rule coupling can move the interband doublon-holon pair excitations outside the Mott gap and restrict the bound states by suppressing the orbital selectivity of the doubly occupied and single-hole states.

DOI: 10.1103/PhysRevB.100.075158

I. INTRODUCTION

The cooperative effect of electron-electron interactions and orbital degeneracy gives rise to a variety of intriguing phenomena in strongly correlated multiorbital systems [1–3]. The interactions in a multiorbital Hubbard model typically consist of three components: an intraorbital Hubbard interaction U, an interorbital Coulomb repulsion U', and the Hund's rule coupling J. Theoretical studies demonstrate that the effective Coulomb repulsion is increased by a finite Hund's rule coupling J, which results in a strong reduction in the critical correlation U_c of the Mott transition [4–6]. Owing to the effect of the Hund's rule coupling, which may greatly suppress interorbital charge fluctuations, an orbital-selective Mott transition (OSMT) will occur, where the carries on a subset of orbitals become localized while the others remain metallic [7].

Four factors may lead to an OSMT in multiorbital systems.

(i) The bandwidth difference plays an essential role in the occurrence of the OSMT, which has been verified by some dynamical mean-field theory (DMFT) investigations [8–11].

(ii) The crystal field splitting reduces the orbital degeneracy to induce the OSMT [4,12–14].

(iii) The next-nearest neighbor (NN) hopping breaks the particle-hole symmetry at half-filling that also benefits the emergence of the OSMT [15];

(iv) The Hund's rule coupling J promotes the OSMT at half-filling by strongly suppressing the coherence scale to block the orbital fluctuations [6,16–18].

The two-orbital Hubbard model is the minimal theoretical model used to study the OSMT [8–20]. In the vicinity of the OSMT, a finite J can lead to fundamentally different low-energy behavior in the two-orbital Hubbard model [21]. A very recent DMFT study [22] found an interesting kind of doublon-holon bound state in the two-orbital Hubbard model when the OSMT occurs. Because the quasiparticle peak of the doublon-holon pair excitation is locked at the Fermi energy when $U = U'$, the OSMT cannot occur, regardless of the difference in the bandwidths of the two orbitals [22].

A doublon (holon) is an excitation in which one particle is added to (removed from) a lattice site with average integer filling. The unique properties of a Mott insulator require the doublon and the holon to form a bound state [23,24]. For the single-band Hubbard model, sharp subpeaks have been found at the inner edges of the Hubbard bands in the metallic phase close to the Mott transition [25–29]. However, the existence of subpeaks in the insulating phase is still a matter of debate [28–32].

In a multiorbital system, there exists a specific relationship between the doublon-holon bound state and the OSMT. The orbital-selective Mott phase (OSMP) between the metallic and insulating phases provides a new perspective for investigating the properties of doublon-holon pair excitations. Multiorbital interactions may also have the capacity to introduce different types of doublon-holon pairs. Very recently, an interesting kind of doublon-holon bound state was found in the OSMP of the two-orbital Hubbard model without the interaction terms for the Hund's rule coupling J [22]. This doublon-holon pair excitation consists of a single-hole state in one band and a doubly occupied state in the other band, which is called an interband doublon-holon bound state. The interband doublon-holon pair excitations provide quasiparticle peaks in the narrow band (NB) only in the presence of a coherent metallic resonance in the wide band (WB) [22]. However, the above findings are mainly based on the assumption that $J = 0$. Hence it is still unclear how the Hund's rule spin exchange

*yunsong@bnu.edu.cn

influences the formation of the interband doublon-holon pair excitations.

In this paper, we study the effect of Hund's rule coupling on the doublon-holon bound states in the two-orbital Hubbard model by using DMFT with the Lanczos method as the impurity solver. We find that some in-gap quasiparticle peaks can appear in the density of states (DOS) of the insulating NB for the OSMP with a smaller Hund's rule coupling and bandwidth ratio. These spectral features indicate the occurrence of the interband doublon-holon bound states, and the orbital selectivity of the doubly occupied state and single-hole state can be found by investigating the excitation spectra of the doublon and the holon. In an OSMP, Hund's rule coupling can split one low-energy quasiparticle peak into two subpeaks, and the energy gap between the two subpeaks is $2J$. The splitting of the quasiparticle peak is mainly caused by the spin-flip and pair-hopping Hund interactions.

Suppression effects on the excitation spectra of the doublon and the holon are found when we increase the Hund's rule coupling. In addition, the distance from the Fermi level to the nearest peak increases linearly with increasing J. As a result, the quasiparticle peaks of the interband doublon-holon pairs may be moved outside the Mott gap, and hence are not easily identified from the high-energy excitations of the Hubbard bands. We also find that the in-gap spectral features disappear completely in the fully insulating phase.

This paper is organized as follows. In Sec. II, we introduce the theoretical model and the DMFT numerical approach. In Sec. III, we calculate the spectral function and the optical conductivity to show the influence of Hund's rule coupling on the doublon-holon bound states. We discuss the conditions for the occurrence of in-gap quasiparticle excitations and the interband feature of the doublon-holon pair excitations. The principal findings of this paper are summarized in Sec. IV.

II. TWO-ORBITAL HUBBARD MODEL AND DYNAMICAL MEAN-FIELD METHOD

We consider the Hamiltonian of the two-orbital Hubbard model:

$$\begin{aligned} H =& -\sum_{\langle ij\rangle l\sigma} t_l d^\dagger_{il\sigma} d_{jl\sigma} - \mu \sum_{il\sigma} d^\dagger_{il\sigma} d_{il\sigma} \\ &+ \frac{U}{2} \sum_{il\sigma} n_{il\sigma} n_{il\bar{\sigma}} + \sum_{i\sigma\sigma'} (U' - \delta_{\sigma\sigma'} J) n_{i1\sigma} n_{i2\sigma'} \\ &+ \frac{J}{2} \sum_{i,l\neq l',\sigma} d^\dagger_{il\sigma} d^\dagger_{il\bar{\sigma}} d_{il'\bar{\sigma}} d_{il'\sigma} \\ &+ \frac{J}{2} \sum_{i,l\neq l',\sigma\sigma'} d^\dagger_{il\sigma} d^\dagger_{il'\sigma'} d_{il\sigma'} d_{il'\sigma}, \end{aligned} \tag{1}$$

where $\langle ij\rangle$ represents the NN sites on a Bethe lattice, $d^\dagger_{il\sigma}$ ($d_{il\sigma}$) is the electron creation (annihilation) operator for the orbital l (=1 or 2) at site i with spin σ, and $n_{il\sigma} = d^\dagger_{il\sigma} d_{il\sigma}$ represents the electron occupation of the orbital l at site i. t_l denotes the NN intraorbital hopping in orbital l, U (U') corresponds to the intraorbital (interorbital) interactions, and J is the Hund's rule coupling. The last two terms represent the pair-hopping and spin-flip Hund interactions, respectively. For systems with spin rotation symmetry, the relationship $U = U' + 2J$ should be kept.

Considering the semicircular DOS of the Bethe lattice, the on-site component of the Green's function of each orbital [$G^{(l)}_{ii}(i\omega_n) = \sum_k G_l(k, i\omega_n)$] satisfies a simple self-consistent relation,

$$\left\{g^{(l)}_0(i\omega_n)\right\}^{-1} = i\omega_n + \mu - t_l^2 G^{(l)}_{ii}(i\omega_n), \tag{2}$$

where g_0 is the noninteracting Green's function [33].

In a DMFT procedure, the lattice Hamiltonian [Eq. (1)] needs to be mapped onto an impurity model with fewer degrees of freedom:

$$\begin{aligned} H_{imp} =& \sum_{ml\sigma} \epsilon_{ml\sigma} c^\dagger_{ml\sigma} c_{ml\sigma} - \mu \sum_{l\sigma} d^\dagger_{l\sigma} d_{l\sigma} \\ &+ \sum_{ml\sigma} V_{ml\sigma} (c^\dagger_{ml\sigma} d_{l\sigma} + d^\dagger_{l\sigma} c_{ml\sigma}) \\ &+ \frac{U}{2} \sum_{l\sigma} n_{l\sigma} n_{l\bar{\sigma}} + \sum_{\sigma\sigma'} (U' - \delta_{\sigma\sigma'} J) n_{1\sigma} n_{2\sigma'} \\ &+ \frac{J}{2} \sum_{l\neq l',\sigma} d^\dagger_{l\sigma} d^\dagger_{l\bar{\sigma}} d_{l'\bar{\sigma}} d_{l'\sigma} + \frac{J}{2} \sum_{l\neq l',\sigma} d^\dagger_{l\sigma} d^\dagger_{l'\sigma'} d_{l\sigma'} d_{l'\sigma}, \end{aligned} \tag{3}$$

where $\epsilon_{ml\sigma}$ denotes the effective parameter of the mth environmental bath of orbital l, and $V_{ml\sigma}$ represents the coupling between the impurity site and its environment baths. The parameters $\epsilon_{ml\sigma}$ and $V_{ml\sigma}$ are determined by performing self-consistent DMFT calculations using an impurity solver.

In our study, we employ the Lanczos solver [34]. The Green's function $G^{(l)}_{imp}(i\omega_n)$ of the impurity model can be expressed as [33,35,36],

$$G^{(l)}_{imp}(i\omega_n) = G^{(+)}_l(i\omega_n) + G^{(-)}_l(i\omega_n), \tag{4}$$

where

$$G^{(+)}_l(i\omega_n) = \cfrac{\langle\phi_0| d_l d^\dagger_l |\phi_0\rangle}{i\omega_n - a^{(+)}_0 - \cfrac{b^{(+)2}_1}{i\omega_n - a^{(+)}_1 - \cfrac{b^{(+)2}_2}{i\omega_n - a^{(+)}_2 - \cdots}}}, \tag{5}$$

$$G^{(-)}_l(i\omega_n) = \cfrac{\langle\phi_0| d^\dagger_l d_l |\phi_0\rangle}{i\omega_n + a^{(-)}_0 - \cfrac{b^{(-)2}_1}{i\omega_n + a^{(-)}_1 - \cfrac{b^{(-)2}_2}{i\omega_n + a^{(-)}_2 - \cdots}}}. \tag{6}$$

In Eq. (1), the two orbitals are nonhybridized. Thus, the self-energy, effective medium functions, and Green's functions are all diagonal with respect to the orbitals. Within multiorbital DMFT calculations [37], the frequency energy is defined as $\omega_n = (2n+1)\pi/\beta$. In our calculations, we choose $\beta = 512$ to assure the accuracy of the self-consistency for the Green's functions, $G_l(i\omega_n) = G^{(l)}_{ii}(i\omega_n) = G^{(l)}_{imp}(i\omega_n)$, especially in the low-energy region. The quasiparticle weights Z_l of different bands can be obtained by

$$Z_l = \left(1 - \frac{\partial}{\partial\omega} \mathrm{Re}\,\Sigma_l(\omega)|_{\omega=0}\right)^{-1} \approx \left(1 - \frac{\mathrm{Im}\,\Sigma_l(i\omega_0)}{\omega_0}\right)^{-1}. \tag{7}$$

Analytic continuation is performed to obtain the real frequency Green's function $G_l(\omega)$ [33]. We calculate the orbital-resolved DOS by $\rho_l(\omega) = -\frac{1}{\pi}\mathrm{Im}G_l(\omega + i\delta)$, where δ is a

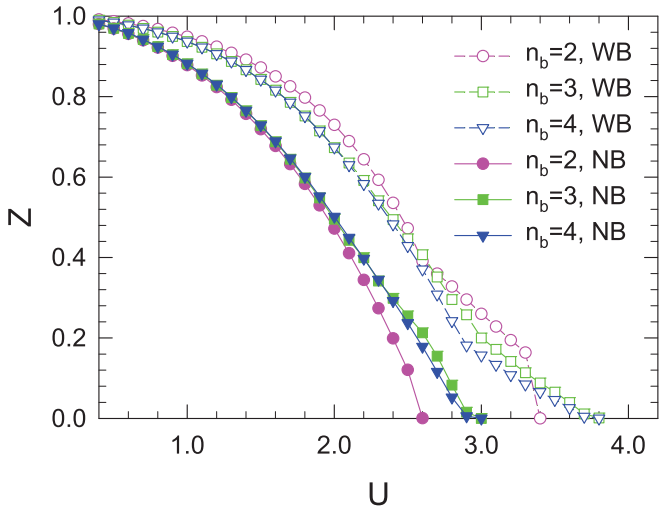

FIG. 1. Effect of the bath size n_b on the critical interactions U_c of the OSMT in the two-orbital Hubbard model. The interaction dependencies of the quasiparticle weight (Z) of the WB (dashed lines and empty symbols) and NB (solid lines and solid symbols) are shown for various bath sizes: $n_b = 2$ (circles), $n_b = 3$ (squares), and $n_b = 4$ (triangles). The same critical values of the OSMT, $U_{c1} = 3.8$ and $U_{c2} = 3.0$, are obtained for the two cases with different bath sizes $n_b = 3$ and $n_b = 4$. The other model parameters are $t_2/t_1 = 0.6$, $J = U/4$, and $U = U' + 2J$. The energies are in units of t_1.

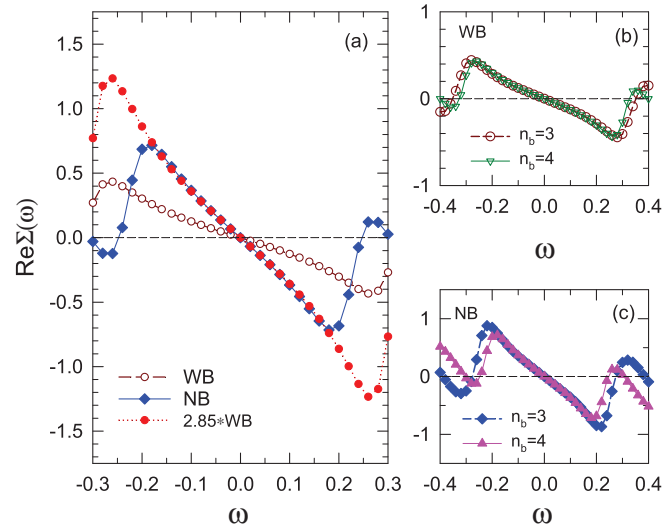

FIG. 2. Common low-energy scale induced by Hund's rule coupling in the vicinity of the OSMT. (a) The self-energies of the two bands has the relation of $\mathrm{Re}\Sigma_2(\omega) = 2.85\mathrm{Re}\Sigma_1(\omega)$ within the energy region $[-0.2, 0.2]$ when the two-orbital Hubbard model is close to the OSMT with $J = 0.5$, $U = 2$, $U = U' + 2J$, and $t_2/t_1 = 0.5$. The self-energies of the WB (b) and the NB (c) are almost the same for $n_b = 3$ and $n_b = 4$ within the corresponding low-energy region.

factor for energy broadening. The orbital-dependent optical conductivity is expressed as

$$\sigma_l(\omega) = \pi \int_{-\infty}^{\infty} d\epsilon D_l(\epsilon) \int_{-\infty}^{\infty} \frac{d\omega'}{2\pi} \rho_l^{(\epsilon)}(\omega') \rho_l^{(\epsilon)}(\omega' + \omega) \times \frac{n_f^{(l)}(\omega') - n_f^{(l)}(\omega' + \omega)}{\omega}, \quad (8)$$

where $n_f(\omega)$ is the Fermi function, and $D_l(\epsilon) = \frac{1}{2\pi t_l}\sqrt{4t_l^2 - \epsilon^2}$ is the semicircular DOS of the Bethe lattice.

III. RESULTS

A. Phase diagram of the OSMT

The existence of the OSMT in a nondegenerate two-orbital Hubbard model is demonstrated by the evolution of the quasiparticle weight Z_l with increasing interactions U when $t_2/t_1 = 0.6$ and $J = U/4$, as shown in Fig. 1. The interaction dependence of Z_l for the cases with $n_b = 3$ and $n_b = 4$ are very similar, which gives the same critical values of the OSMT: $U_{c1} = 3.8$ for the WB and $U_{c2} = 3.0$ for the NB. For the two-orbital Hubbard model with parameters close to the OSMT, a common low-energy scale is found when the Hund's rule coupling is strong [21]. As shown in Fig. 2(a), the self-energy of the NB is approximately equal to the product of the self-energy of the WB and a certain constant, i.e., $\mathrm{Re}\Sigma_2(\omega) \approx \alpha \mathrm{Re}\Sigma_1(\omega)$, in the low-energy region $[-0.2, 0.2]$. The constant α is found to be 2.85 when $U = 2$ and $J = 0.5$. In Figs. 2(b) and 2(c), it is also shown that there is no obvious change in the self-energy for the cases with $n_b = 3$ and $n_b = 4$ for both the WB and the NB in the low-energy region. Our findings support the prediction that the effective bath size is doubled in the vicinity of the OSMT in the two-orbital Hubbard model.

In agreement with the prediction of some previous DMFT calculations [16], our study shows that one can accurately determine the critical points of Mott transitions in the two-orbital Hubbard model by using the Lanczos solver with a limited bath size. Therefore, we could comprehensively investigate the influence of different model parameters on the phase diagram of the two-orbital Hubbard model, especially the Hund's rule coupling J.

In Fig. 3, we compare the phase diagrams of the two-orbital Hubbard model with different Hund's rule couplings. For the cases with a small J, the OSMT occurs only if the orbital difference meets a certain requirement. For example, the appearance of the OSMP requires $t_2/t_1 \leqslant 0.6$ when $J = U/8$, as shown in Fig. 3(b). However, the OSMP can exist for any bandwidth ratio when the Hund's rule coupling is sufficiently strong. As illustrated in Fig. 3(d), a boundary for the existence of the OSMT is presented, which clearly shows that the Hund's rule coupling significantly promotes the OSMT. There is no OSMT for any nonzero bandwidth in both bands when $J = 0$. When $J = 0$, the quasiparticle peaks of the interband doublon-holon pairs will be locked at the Fermi level, leading to the simultaneous appearance of the Mott transition for both bands, regardless of the difference in bandwidths [22].

B. Quasiparticle excitations in the OSMP

We find in the OSMP that some low-energy quasiparticle peaks appear inside the Mott gap of the NB when the Hund's rule coupling is sufficiently small. Figure 4 shows the DOS of the NB and the WB of the two-orbital Hubbard model in an OSMP. Four peaks of quasiparticle excitations are found

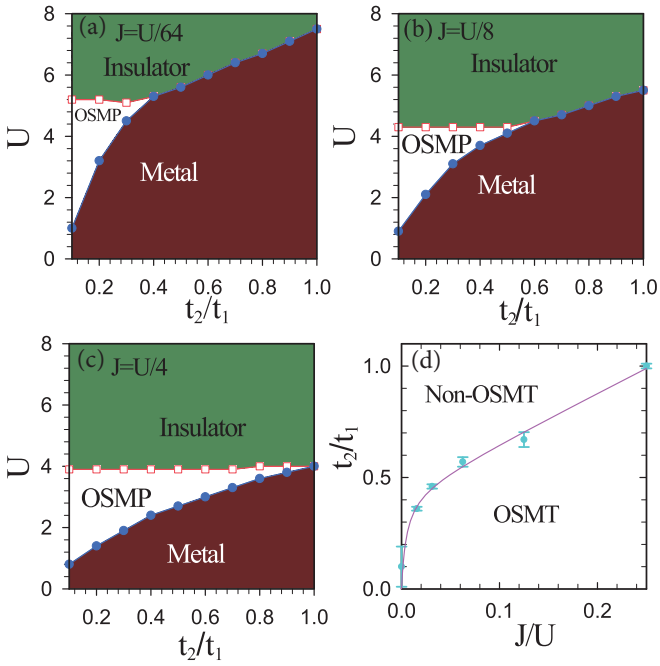

FIG. 3. Phase diagrams of the two-orbital Hubbard model with various Hund's rule couplings: $J = U/64$ (a), $J = U/8$ (b), and $J = U/4$ (c). Both the critical values U_{c1} and U_{c2} for the WB and the NB decrease as the Hund's rule coupling increases due to the enhancement in the Coulomb interactions caused by J. When the Hund's rule coupling is sufficiently strong ($J \geqslant U/4$), the OSMT can occur for any bandwidth ratio t_2/t_1. (d) Dependence of the boundary between the OSMT region and non-OSMT region on the Hund's rule coupling. As J decreases, a significant decline in the threshold of the ratio t_2/t_1 is observed, which drops to zero when $J = 0$. Thus, there is no OSMT for any nonzero bandwidth in both bands when $U = U'$ and $J = 0$.

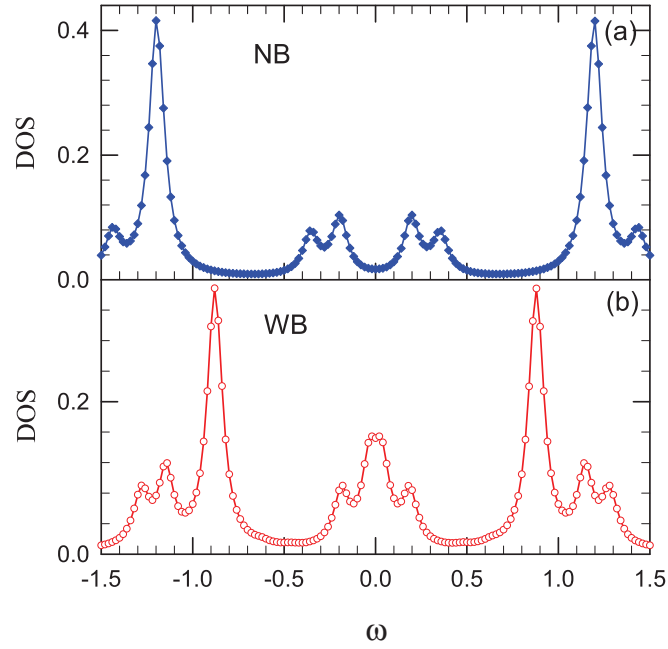

FIG. 4. DOS showing the low-energy quasiparticle states in the OSMP of the nondegenerate two-orbital Hubbard model with a small Hund's rule coupling J. In the low-energy region around the Fermi level, the DOS of the NB (a) and the WB (b) are presented for the OSMP with $U = 5.1$, $J = U/64 \approx 0.08$, $t_2/t_1 = 0.2$, and $U = U' + 2J$. The corresponding OSMT critical interactions are $U_{c1} = 5.3$ and $U_{c2} = 3.2$. The OSMP is very close to the insulating transition point. Four quasiparticle peaks are found close to the Fermi level in the NB, and the corresponding excitations carry energies of $E = \pm 0.17$ and ± 0.34, respectively. The energies are in units of t_1, and the energy broadening is $\delta = 0.05$.

close to the Fermi level in the NB, as shown in Fig. 4(a). Here, the model parameters are $U = 5.1$, $J = 0.08$, $t_2/t_1 = 0.2$, and $U = U' + 2J$. The corresponding Mott critical values for the WB and the NB are obtained as $U_{c1} = 5.3$ and $U_{c2} = 3.2$, respectively. Therefore, the system with $U = 5.1$ is in an OSMP, which is close to the insulating transition point U_{c1}.

In the NB, the four peaks are symmetrically located around the Fermi level, carrying energies of $E = \pm 0.19$ and ± 0.36. It is important to note that the energy splitting between the two nearby quasiparticle peaks with positive (negative) energy is $\Delta = 0.17$, which is approximately equal to $2J$ ($J = 0.08$). In the WB, we can also find two low-energy peaks at the two sides of the center coherent peak, as shown in Fig. 4(b). As with the two inner quasiparticle peaks in the NB, the two low-energy peaks in the WB carry energies of $E = -0.19$ and $E = 0.19$. This energy association implies that the quasiparticle bound states may not be orbitally independent.

Numerous numerical calculations have been carried out for the two-orbital Hubbard model with various model parameters, and we find that the energies carried by the quasiparticle peaks do not change with changes in the bandwidth ratio t_2/t_1 when the Hund's rule coupling J is fixed.

Low-energy quasiparticle excitations may be observed by the orbital-resolved optical conductivity of multiorbital correlated compounds. In Fig. 5, we present the optical conductivities of the WB and the NB obtained for different phases of the two-orbital Hubbard model. The quasiparticle states contribute significantly to the optical conductivity in the OSMP. As expected, the optical conductivity of the NB exhibits a significant feature in the low-energy region, presenting the transfer of spectral weight between the quasiparticle excitations appearing in the NB. Meanwhile, the Drude weight in the optical conductivity of the WB indicates that the WB is metallic. In contrast, Drude peaks are shown for both optical conductivities of the two bands in the metallic phase [Fig. 5(c)].

The Mott transition occurs in the WB when $U > U_{c1}$, accompanied by the vanishing of the coherent metallic resonance and the quasiparticle peaks. The orbital-dependent optical conductivity can also illustrate the disappearance of the quasiparticle peaks in the insulating phase, as shown in Fig. 5(b). Owing to the absence of low-energy excitations, Mott gaps are clearly shown in the optical conductivities for both bands [Fig. 5(b)]. This finding is of great significance for solving the dispute regarding whether there are subpeaks in the insulating phase of the single-band Hubbard model.

C. Effect of J on the quasiparticle excitations

Núñez-Fernández *et al.* studied the low-energy bound states in a simplified two-orbital Hubbard model [22]. Without

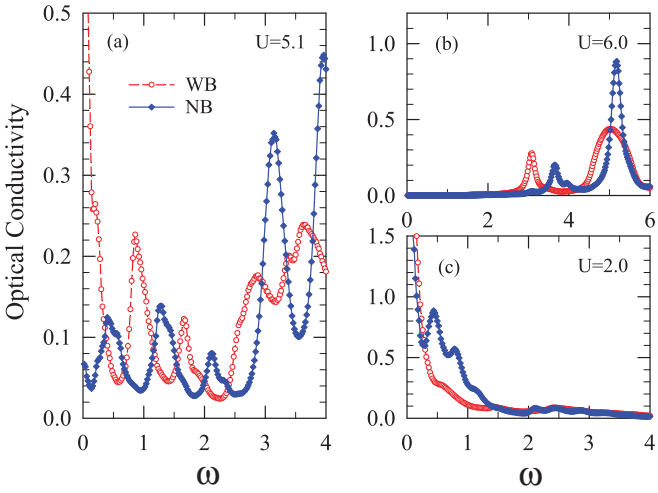

FIG. 5. Manifestation of the emergence of low-energy bound quasiparticle states by orbital-resolved optical conductivity. We compare the optical conductivities of the NB and the WB for different phases: the OSMP (a), the insulating phase (b), and the metallic phase (c). In the OSMP, the low-energy peaks in the NB optical conductivity (solid line and solid symbols) indicate the transfer of spectral weight between the quasiparticle peaks of the low-energy bound excitations appearing in the NB. These low-energy in-gap excitations completely disappear in the insulating phase. The other model parameters are the same as those in Fig. 4.

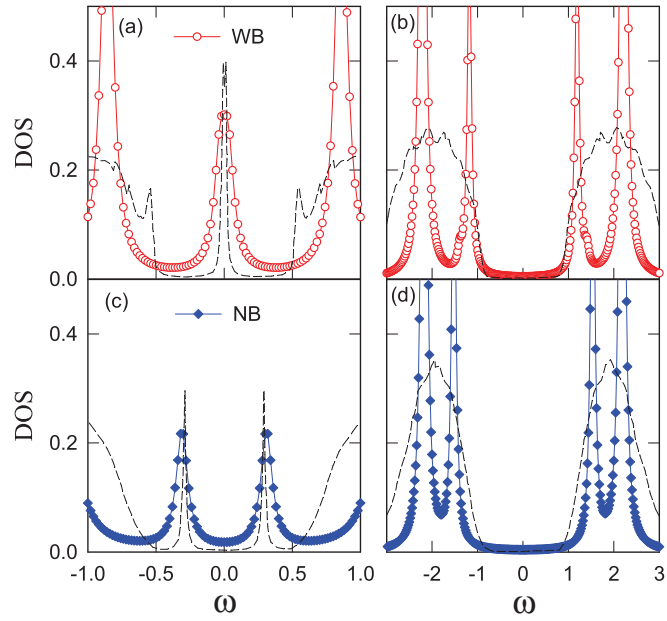

FIG. 6. Low-energy quasiparticle peaks with broken spin-symmetry. Left panels: The low-energy DOS of the WB (a) and the NB (c) in the OSMP when $J = 0$, $U = 3$, and $U - U' = 0.3$. Two quasiparticle peaks are found in the NB, located approximately at $\omega = -0.3$ and $\omega = 0.3$. Right panels: The DOS of the WB (b) and the NB (d) in the insulating phase when $J = 0$, $U = 4.0$, and $U - U' = 0.3$. The quasiparticle peaks in the NB disappear with the vanishing of the central resonance peak in the WB. Compared with the results obtained by the DMFT + DMRG (black dashed lines) [22], very good agreement is achieved. The other model parameters are $t_1 = 0.5$ and $t_2 = 0.25$.

the Hund's rule coupling terms, this model is still able to show the OSMT, but the spin rotation symmetry is broken when $U \neq U'$. The authors found that a finite DOS at the Fermi energy in the WB is correlated with the emergence of well-defined quasiparticle states at the excited energy $\Delta = U - U'$ in the insulating NB [22]. For a comparison with their results, we also calculate the DOS of the two-orbital Hubbard model with $J = 0$ and $U \neq U'$. Our results are in good agreement with the results obtained by using DMFT with the density-matrix renormalization group method as the impurity solver [22], as shown in Fig. 6. Our finding indicates that the splitting of quasiparticle excitations is caused by Hund's rule coupling. In the NB, as shown in Fig. 6(c), there are only two quasiparticle peaks when J is absent. In addition, there is no quasiparticle excitation in both the WB and the NB for the fully insulating phase, as shown in Figs. 6(b) and 6(d). Núñez-Fernández *et al.* predicted that these quasiparticle excitations are interband holon-doublon bound states [22].

To understand the effects of the different terms in the Hund interaction Hamiltonian on the energy splitting of quasiparticle excitations, we compare the low-energy DOS of two different models with different Hund interactions, as shown in Fig. 7. When only the interorbital density-density Hund interactions are considered, there are only two quasiparticle peaks in the NB, which are located at $\omega = \pm 0.265$. We suppose that the energies of the quasiparticle peaks may be determined by $D = U - U' + J$. The interaction parameters are $U - U' = 0.16$, $J = 0.08$, and $U = 5.1$ ($U - U' = 2J$). Our prediction is in good agreement with the findings of Ref. [22] ($J = 0$ and $D = U - U' = 0.3$), where the two peaks carry energies of 0.3 and -0.3, as shown in Fig. 6(c).

Four quasiparticle peaks appear in the NB when the influences of the full Hund interactions are considered. As shown in Fig. 7(b), the energies carried by the four quasiparticles in the NB are 0.36, 0.19, -0.19, and -0.36. Our results indicate that the energy splitting of the interband holon-doublon bound states is mainly caused by the spin-flip and pair-hopping Hund interactions. As a special type of double-hopping term, the pair-hopping Hund's rule coupling can move two electrons from one orbital to another simultaneously, which contributes to the occurrence of interband doublon-holon pairs and the transition between different interband bound states. Similarly, the spin-flip exchange interaction also has a significant effect on the interorbital doublon-holon bound states because it represents a particular kind of double-hopping term between the two orbitals. The transverse (spin-flip and pair-hopping) Hund's rule couplings enhance the electronic interactions and spin fluctuations, resulting in the splitting of the doublon-holon excitations. The interplay between the split doublon-holon bound states and the dependence of the splitting energy on effective doublon-holon pair interactions require further investigations.

As mentioned in the previous subsection, there might also exist some low-energy quasiparticle peaks in the WB. However, the WB is in the metallic phase, and there is a resonance peak at the Fermi level. Therefore, distinguishing the low-energy quasiparticle excitations with the central resonance peak is difficult. We find that the overlap between the

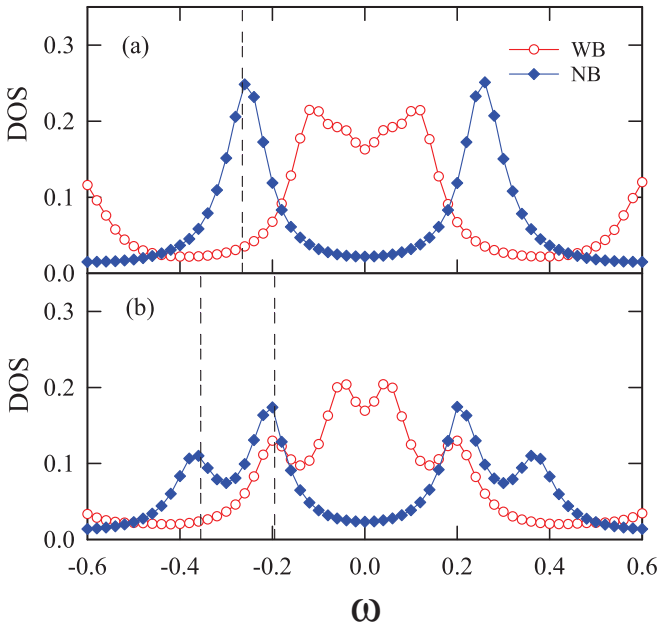

FIG. 7. Influence of the different interaction terms of the Hund's rule coupling Hamiltonian on the quasiparticle excitations: (a) when only the interorbital density-density Hund interactions are considered, and (b) when the spin-flip and pair-hopping Hund interactions are also included. The positions of the in-gap quasiparticle peaks in the NB are indicated by the dashed lines in the negative-energy region. It is obvious that the splitting of the quasiparticle excitations is mainly driven by the spin-flip and pair-hopping Hund interactions. The model parameters are the same as those in Fig. 4.

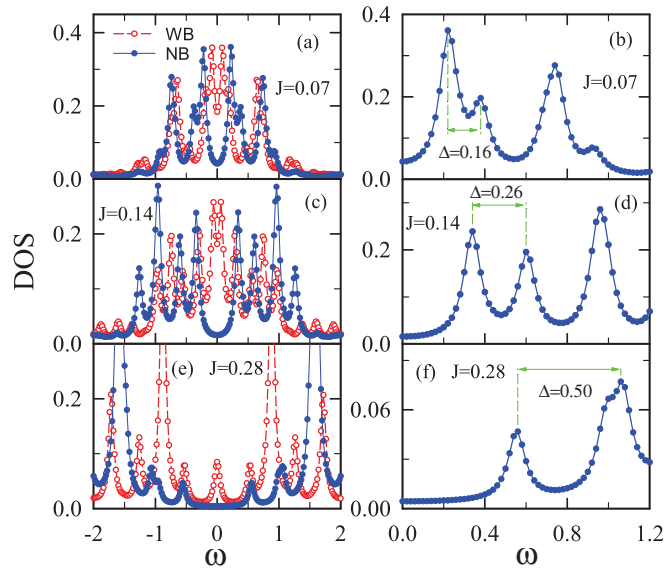

FIG. 8. Quasiparticle excitations are split by Hund's rule coupling in the OSMP. Left panels: The DOS of the WB and the NB for different Hund's rule couplings: $J = 0.07$ (a), $J = 0.14$ (c), and $J = 0.28$ (e). Right panels: A one-to-one correspondence with the left panels. The energy splitting between the quasiparticle peaks is shown in the low-energy DOS of the NB. The two-orbital Hubbard model remains in the OSMP with $t_2/t_1 = 0.2$ and $U = 4.5$. The positions of the quasiparticle peaks increase linearly with increasing Hund's rule coupling. A linear dependence of the energy splitting between the peaks on J is also found.

interband bound states with the resonance peak is reduced when the spin-flip and pair-hopping Hund interactions are included. Also shown in Fig. 7(b), two quasiparticle peaks are found at ± 0.19 in the WB, which have the same energies as the two inner peaks in the NB.

We further study the relation between the energy splitting Δ and J. We focus on the two-orbital Hubbard model with full Hund's rule coupling. In Fig. 8, from top to bottom, Hund's rule coupling increases from $J = 0.07$ to $J = 0.14$ and finally to $J = 0.28$, and the intraorbital interactions are fixed as $U = 4.5$. In the left panels, the DOS of the WB and the NB clearly show that the two-orbital Hubbard model remains in the OSMP with the change in the Hund's rule coupling. Correspondingly, in the right panels, we indicate the energy splitting Δ between the two nearby quasiparticle peaks in the NB for the three cases with different J. It is shown that the splitting energy increases linearly with increasing J, satisfying the relation $\Delta = 2J$.

In addition, our study also suggests that there also exists a linear relationship between the position of the quasiparticle peak and the Hund's rule coupling J. When the Hund's rule coupling increases from $J = 0.14$ to $J = 0.28$, the energy carried by the inner peak is found to increase from $\omega = 0.26$ to $\omega = 0.50$.

It is worth noticing that a small bandwidth ratio t_2/t_1 is an essential condition for the emergence of the low-energy quasiparticle peaks in the OSMP of the two-orbital Hubbard model. Many earlier DMFT studies focused on the OSMT with a bandwidth ratio of $t_2/t_1 = 0.5$ only, which may be the main reason why the feature of the quasiparticle peaks was missing. Based on the phase diagrams shown in Fig. 3, to find the OSMP for the cases with $t_2/t_1 = 0.5$, the Hund's rule coupling must be larger than 0.5. The quasiparticle peaks are predicted to appear in the high-energy region ($U - U' > 1.0$). Thus, it would be difficult to distinguish them from the excitations in the Hubbard bands.

D. Excitation spectra of the doublon and the holon

The spectrum function has well-defined quasiparticle peaks in the low-energy region when the two-orbital Hubbard model is in the OSMP with a small Hund's rule coupling. To characterize the feature of these quasiparticle excitations, we focus primarily on the orbital-resolved excitation spectrum of the doublon $D_l(\omega)$, which is defined as

$$D_l^{(-)}(\omega) = -\frac{1}{\pi}\mathrm{Im}\langle b_l^\dagger(\omega - H + i\delta^+)^{-1}b_l\rangle, \qquad (9)$$

where the doublon operator [28] $b_l^\dagger = n_{l\downarrow}d_{l\uparrow}^\dagger$ creates a doubly occupied state in orbital l.

The excitation spectrum of the doublon within the negative low-energy region is plotted in Fig. 9 for the two-orbital Hubbard model with different Hund's rule couplings: $J = 0.14$ (left panel) and $J = 0.28$ (right panel). Obviously, the doublon spectrum function of the WB is much stronger than that of the NB, which suggests that the doubly occupied states prefer to stay in the WB. In addition, the excitation spectrum

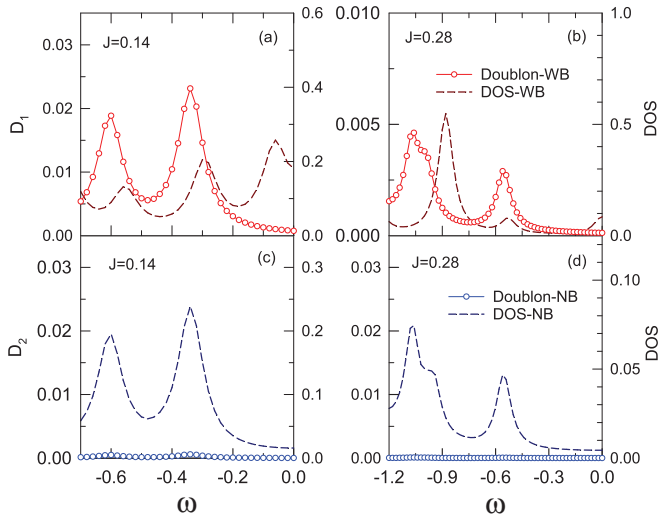

FIG. 9. Orbital selectivity of the doubly occupied states in the OSMP. The excitation spectra of the doublon in the WB [panels (a) and (c)] and the NB [panels (b) and (d)] are shown by the solid lines with empty symbols, for the OSMP with different Hund's rule couplings $J = 0.14$ and $J = 0.28$. For a comparison, the DOS of the two bands are also presented by the dashed lines. The doublon spectrum of the WB is significantly larger than that of the NB, indicating that the doubly occupied states prefer to stay in the WB. The energies of the in-gap peaks in the DOS of the NB correspond to the positions of the peaks in the doublon spectrum. The other model parameters are $U = 4.5$, $t_2/t_1 = 0.2$, and $U = U' + 2J$.

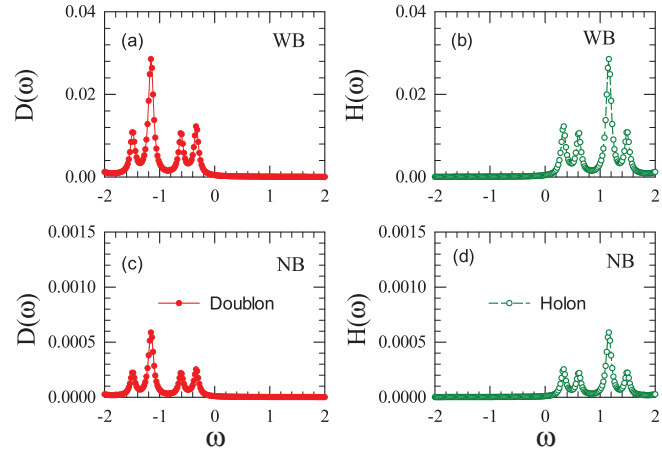

FIG. 10. Excitation spectra of the doublon (left panels) and holon (right panels) for the WB and the NB in the OSMP with $J = 0.14$, $t_2/t_1 = 0.2$, $U = 4.5$, and $U = U' + 2J$. The spectrum weight of the doublon (holon) of the wide band is approximately 2 orders higher than the corresponding spectrum weight of the NB.

is found to decrease with increasing Hund's rule coupling, which indicates that strong Hund's rule coupling suppresses the orbital selectivity of the doubly occupied state.

Moreover, a specific correlation between the two bands is also observed for the first time, where the energies carried by the quasiparticle excitations in the NB are determined by the positions of the peaks shown in the excitation spectrum of the doublon of the WB. As shown in Figs. 9(a) and 9(c), in the negative energy region when $U = 4.5$ and $J = 0.14$, there are two peaks in the excitation spectrum of the doublon of the WB (red solid line with circles), which carry energies of $\omega = -0.32$ and $\omega = -0.59$, respectively. The DOS of the NB also has two peaks (blue dashed line), and the positions of these two peaks correspond exactly to the peaks in the doublon spectrum of the WB.

This investigation provides insight into the intrinsic orbital-selective characteristics of the doubly occupied states. Furthermore, the interorbital correlation between the doublon spectrum and the DOS implies that the quasiparticle excitation should be formed by the doublon and holon in different orbitals, which is just the interband doublon-holon bound state [22]. We predict that the interband doublon-holon pair with negative energy should consist of a doublon in the WB and a hole in the NB. To confirm this hypothesis, we also need to further study the orbital selectivity of the single-hole state.

Correspondingly, the excitation spectrum of the holon $H_l^{(+)}(\omega)$ can be expressed by the following equation:

$$H_l^{(+)}(\omega) = -\frac{1}{\pi}\mathrm{Im}\langle h_l(\omega - H + i\delta^+)^{-1}h_l^\dagger\rangle, \qquad (10)$$

where $h_l^\dagger = (1 - n_{l\downarrow})d_{l\uparrow}$ presents the holon operator [28] of orbital l.

In a half-filled system with particle-hole symmetry, the holon spectrum function $H_l^{(+)}(\omega)$ is not independent. Based on the particle-hole transformation, we can find that there is an asymmetric relationship, $D_l^{(-)}(-\omega) = H_l^{(+)}(\omega)$, under the transition $\omega \to -\omega$.

In Fig. 10, we compare the excitation spectra of the doublon and the holon in the OSMP. As expected, the excitation spectrum of a hole in the positive-energy region matches the spectrum of the doubly occupied state in the negative-energy region. A basic feature of the interband doublon-holon bound state is found, where the pair excitation also shows an asymmetric relation under the energy transition $\omega \to -\omega$. The interband doublon-holon pair with positive (negative) energy consists of a holon (doublon) in the WB and a doublon (holon) in the NB. These theoretical predictions need to be tested and verified by experiments. Additionally, the relationship between the effective doublon-holon pair interaction and Hund's rule coupling in the multiorbital Hubbard model still needs to be explored by further research.

IV. CONCLUSION

We study the effect of Hund's rule spin exchange on the doublon-holon pair excitations in the two-orbital Hubbard model by using DMFT with the Lanczos method as the impurity solver. Our calculations show that low-energy quasiparticle peaks occur in the DOS of the OSMP if both the Hund's rule coupling J and the bandwidth ratio t_2/t_1 are small enough. These low-energy excitations are the interband doublon-holon bound states, in which the doublon is located in one band while the holon is in the other band.

The spin-flip and pair-hopping Hund interactions can divide one quasiparticle peak into two peaks. The linear relation $\Delta = 2J$ has been confirmed between the energy gap and the Hund's rule coupling. In addition, the energies carried by the

quasiparticle peaks are also controlled by the Hund's rule coupling.

There exists a direct correspondence between the energies of the quasiparticle peaks in one band and the positions of the peaks in the excitation spectrum of the doublon for the other band. Our study demonstrates that the interband doublon-holon pair with positive (negative) energy consists of a holon (doublon) in the WB and a doublon (holon) in the NB.

When the Hund's rule coupling is strong, the interband doublon-holon pair excitations are suppressed with a significant reduction in the excitation spectra of the doublon and the holon. In addition, the low-energy quasiparticle peaks are moved to Hubbard bands and hence are inefficiently identified. The interband doublon-holon bound states disappear completely in the fully insulating phase.

ACKNOWLEDGMENTS

The computational resources utilized in this research were provided by Shanghai Supercomputer Center. The work is supported by the the National Natural Science Foundation of China (NSFC), under Grants No. 11174036 and No. 11474023. S.F. is supported by the National Key Research and Development Program of China under Grant No. 2016YFA0300304 and the NSFC under Grants No. 11574032 and No. 11734002.

[1] M. Imada, A. Fujimori, and Y. Tokura, Rev. Mod. Phys. **70**, 1039 (1998).
[2] G. Kotliar, S. Y. Savrasov, K. Haule, V. S. Oudovenko, O. Parcollet, and C. A. Marianetti, Rev. Mod. Phys. **78**, 865 (2006).
[3] G. Rohringer, H. Hafermann, A. Toschi, A. A. Katanin, A. E. Antipov, M. I. Katsnelson, A. I. Lichtenstein, A. N. Rubtsov, and K. Held, Rev. Mod. Phys. **90**, 025003 (2018).
[4] P. Werner and A. J. Millis, Phys. Rev. Lett. **99**, 126405 (2007).
[5] A. H. Nevidomskyy and P. Coleman, Phys. Rev. Lett. **103**, 147205 (2009).
[6] A. Georges, L. de' Medici, and J. Mravlje, Annu. Rev. Condens. Matter Phys. **4**, 137 (2013).
[7] V. I. Anisimov, I. A. Nekrasov, D. E. Kondakov, T. M. Rice, and M. Sigrist, Eur. Phys. J. B **25**, 191 (2002).
[8] A. Koga, N. Kawakami, T. M. Rice, and M. Sigrist, Phys. Rev. Lett. **92**, 216402 (2004)
[9] A. Koga, N. Kawakami, T. M. Rice, and M. Sigrist, Phys. Rev. B **72**, 045128 (2005).
[10] L. de' Medici, A. Georges, and S. Biermann, Phys. Rev. B **72**, 205124 (2005).
[11] Y. Song and L.-J. Zou, Phys. Rev. B **72**, 085114 (2005).
[12] L. de' Medici, S. R. Hassan, M. Capone, and X. Dai, Phys. Rev. Lett. **102**, 126401 (2009).
[13] Y. Song and L.-J. Zou, Eur. Phys. J. B **72**, 59 (2009).
[14] E. Jakobi, N. Blümer, and P. van Dongen, Phys. Rev. B **87**, 205135 (2013).
[15] Y. K. Niu, J. Sun, Y. Ni, and Y. Song, Phys. B (Amsterdam, Neth.) **539**, 106 (2018).
[16] A. Liebsch, Phys. Rev. Lett. **95**, 116402 (2005).
[17] L. de' Medici, Phys. Rev. B **83**, 205112 (2011).
[18] J. Sun, Y. Liu, and Y. Song, Acta Phys. Sin. **64**, 247101 (2015).
[19] T. A. Costi and A. Liebsch, Phys. Rev. Lett. **99**, 236404 (2007).
[20] L. de' Medici, J. Mravlje, and A. Georges, Phys. Rev. Lett. **107**, 256401 (2011).
[21] M. Greger, M. Kollar, and D. Vollhardt, Phys. Rev. Lett. **110**, 046403 (2013).
[22] Y. Núñez-Fernández, G. Kotliar, and K. Hallberg, Phys. Rev. B **97**, 121113(R) (2018).
[23] X.-J. Han, Y. Liu, Z.-Y. Liu, X. Li, J. Chen, H.-J. Liao, Z.-Y. Xie, B. Normand, and T. Xiang, New J. Phys. **18**, 103004 (2016).
[24] P. Phillips, Rev. Mod. Phys. **82**, 1719 (2010).
[25] R. G. Leigh and P. Phillips, Phys. Rev. B **79**, 245120 (2009).
[26] Y. Yamaji and M. Imada, Phys. Rev. B **83**, 214522 (2011).
[27] S. Zhou, Y. Wang, and Z. Wang, Phys. Rev. B **89**, 195119 (2014).
[28] S.-S. B. Lee, J. von Delft, and A. Weichselbaum, Phys. Rev. Lett. **119**, 236402 (2017).
[29] S.-S. B. Lee, J. von Delft, and A. Weichselbaum, Phys. Rev. B **96**, 245106 (2017).
[30] S. Nishimoto, F. Gebhard, and E. Jeckelmann, J. Phys. Condens. Matter **16**, 7063 (2004).
[31] E. Gull, D. R. Reichman, and A. J. Millis, Phys. Rev. B **82**, 075109 (2010).
[32] M. Granath and J. Schött, Phys. Rev. B **90**, 235129 (2014).
[33] A. Georges, G. Kotliar, W. Krauth, and M. J. Rozenberg, Rev. Mod. Phys. **68**, 13 (1996).
[34] E. Dagotto, Rev. Mod. Phys. **66**, 763 (1994).
[35] M. Caffarel and W. Krauth, Phys. Rev. Lett. **72**, 1545 (1994).
[36] M. Capone, L. de' Medici, and A. Georges, Phys. Rev. B **76**, 245116 (2007).
[37] R. Arita and K. Held, Phys. Rev. B **72**, 201102(R) (2005).